SPANDIDOS PUBLICATIONS

ONCOLOGY LETTERS 18: 4278-4287, 2019

Diosgenin inhibits the epithelial-mesenchymal transition initiation in osteosarcoma cells via the p38MAPK signaling pathway

HUAMING HUANG[1,2], CHAO NIE[1], XIAOKANG QIN[3], JIE ZHOU[1] and LEI ZHANG[1]

[1]Department of Research Office, Jiangsu Health Vocational College, Nanjing, Jiangsu 211800;
[2]Department of Orthopedics, Xishan People's Hospital of Wuxi, Wuxi, Jiangsu 214015;
[3]Jiangsu KeyGEN BioTECH Co., Ltd., Nanjing, Jiangsu 211100, P.R. China

Received September 21, 2018; Accepted June 13, 2019

DOI: 10.3892/ol.2019.10780

Abstract. Diosgenin is an important basic raw material for the production of steroid hormone drugs. It can be isolated and purified from a variety of traditional Chinese medicines or plants. Modern molecular biological studies have shown that diosgenin inhibits various tumor cells migration and invasion ability to varying degrees *in vitro* and *in vivo*. The aim of the present study was to observe the inhibitory effects of diosgenin on the invasive and metastatic capabilities of osteosarcoma cells and to determine the association between the effects of diosgenin on the epithelial-mesenchymal transition (EMT). Wound healing and Transwell assays were used to observe the inhibitory effects of diosgenin on the invasion and migration of two osteosarcoma cell lines. Immunofluorescence was used to observe changes in transforming growth factor β1 (TGF-β1) protein expression levels in the osteosarcoma cells following drug administration. EMT-associated proteins, including TGFβ1, E-cadherin and vimentin were detected by western blotting, which demonstrated that the drug may inhibit the initiation of EMT in osteosarcoma cells. Western blot analysis of the expression of all the proteins in the mitogen-activated protein kinase (MAPK) pathway demonstrated that the drug inhibited the MAPK signaling pathway. The primary mechanism of action of diosgenin was the inhibition of the phosphorylated p38 (pP38) protein. Through a combination of inhibitors of the p38MAPK signaling pathway and detection of the downstream EMT marker protein E-cadherin by quantitative PCR, pP38 was confirmed to be a target of diosgenin in the inhibition of EMT in the osteosarcoma cells via the MAPK molecular signaling pathway. Diosgenin may exhibit utility as an auxiliary drug for the clinical reduction of metastasis in patients with osteosarcoma.

Correspondence to: Professor Lei Zhang, Department of Research Office, Jiangsu Health Vocational College, 69 Huangshanling Road, Pukou, Nanjing, Jiangsu 211800, P.R. China
E-mail: jsjkzl@outlook.com

Key words: diosgenin, osteosarcoma, epithelial-mesenchymal transition, invasion, migration

Introduction

Osteosarcoma is a malignant tumor of skeletal origin, and its incidence remains high among primary malignant bone tumors (1). Patients are primarily adolescents, and osteosarcoma is associated with a high degree of malignancy, particularly metastasis to the lungs during the early stages. Cases of osteosarcoma, in particular cases with evidence of lung metastasis, are associated with a poor prognosis (2). Osteosarcoma exerts a large toll on mental health on patients and their families. In recent years, surgical treatment and neoadjuvant chemotherapy have improved the treatment of this disease (3,4). Radiotherapy and chemotherapy combined with limb salvage surgery have replaced amputation surgery and have become the primary surgical method for treating patients with osteosarcoma (5). As therapeutic radiotherapy and chemotherapy regimens may not effectively remove all tumor cells, 20-40% of patients undergoing this treatment may still die of metastasis, and metastases are one of the primary factors affecting the survival rate of patients with osteosarcoma (6). With the discovery of an increasing number of molecular mechanisms that can mediate the invasion and metastasis of osteosarcoma (7-9), identifying novel drugs or therapeutic regimens to inhibit these processes and improve the survival rate of patients has become the primary task for improving the current clinical treatment options available.

Diosgenin is a hydrolysate of dioscin, which is an important basic raw material necessary for the production of steroid hormone drugs (10). Diosgenin is an important steroidal sapogenin and is widely distributed in plants of the *Dioscoreae*, *Liliaceae*, *Rosaceae* and *Caryophyllaceae* genera and a number of other plants (11). Diosgenin is one of the active ingredients in a variety of Chinese medicines, and it has anti-inflammatory, antidiabetic, antithrombotic, antiallergic and antiviral properties (12-16). A number of studies have shown that diosgenin inhibits tumor cells by interfering with apoptosis and autophagy of tumor cells (17-22). However, to the best of our knowledge, there are no studies investigating the role of diosgenin in the invasion and migration of osteosarcoma cells, and the exact mechanisms underlying its effects remain unknown., and the exact mechanisms underlying its effects remain unknown.

The epithelial-mesenchymal transition (EMT) is a process cancerous cells undergo in which cells with epithelial-like

morphologies undergo morphological and molecular changes to attain a mesenchymal-like morphology and thus becoming more migratory (23). Cells lose their polarity, contact with surrounding cells, the extracellular matrix is reduced and cellular migration and motility are increased. In addition, the phenotype of these cells changes, and characteristics associated with interstitial cells appear (24). These changes enhance the invasive and migratory capacity of tumor cells (25). EMT is one of the transformations by which tumor cells can acquire the ability to migrate and is an important process in tumor cell infiltration and metastasis (26,27). An increasing number of experimental studies have shown that the initiation of EMT serves a critical role in the invasion and metastasis of osteosarcoma (9,28,29). The present study applied diosgenin to two different osteosarcoma cell lines to observe the effects of this drug on the invasion and migration of the cells, and the mechanism of action was further explored in relation to the inhibition of EMT initiation in tumor cells.

Materials and methods

Chemicals and reagents. Diosgenin, purity >90% was identified in Nanjing Zelang Technology Co., Ltd. by HPLC and was purchased from Nanjing Zelang Medical Technology Co., Ltd. (cat. no. ZL20170702014). A First Strand cDNA Synthesis kit was obtained from Thermo Fisher Scientific, Inc., fetal bovine serum (FBS) was purchased from ExCell Biology, Inc., TRIzol® was purchased from Invitrogen; Thermo Fisher Scientific, Inc., chloroform and isopropanol were purchased from Nanjing Chemical Reagent Co., Ltd. and 0.25% trypsin-EDTA, PBS, total protein extraction kit, Braford assay kit, 5X SDS-PAGE protein loading buffer solution, SDS-PAGE gel preparation kit, prestained protein molecular weight ladder, 10X Tris-glycine protein electrophoresis buffer, Coomassie blue staining protein detection kit, phosphorylated p38 (pP38) inhibitor SB203580, 10X electrotransfer buffer solution, Ponceau staining solution, western blotting primary antibody diluent, a western blotting secondary antibody diluent, enhanced chemiluminescent detection kit, internal reference primary antibody (anti-GAPDH; cat. no. KGAA002-1; dilution, 1:200), secondary antibody, and developing and fixing reagents were all purchased from KeyGen Biotechnology Co., Ltd.

Cell culture. Human osteosarcoma MG63 and U2OS cells were donated by Jiangsu Health Vocational College (Nanjing, China). The MG63 and U2OS cells were treated with 90% minimal essential medium supplemented with 10% FBS or 90% complete DMEM supplemented with 10% FBS, respectively. The cells were cultured at 37˚C in 5% CO_2. The culture medium was replaced every 2 days.

MTT assay and calculation of the cellular IC_{50}. Cells in the logarithmic growth phase were collected, and the two cell lines were prepared in cell suspensions at a concentration of $5x10^4$ cells/ml. The cells were added to 96-well cell culture plates (100 μl per well) and placed in a 37˚C, 5% CO_2 incubator for 24 h. Diosgenin diluted to various concentrations in complete medium (200, 100, 50, 25, 12.5 and 6.25 μM) was added to the 96-well medium. Untreated cells were the negative control group. The culture plates were placed in a 37˚C, 5% CO_2 incubator for 24 h after which MTT staining was performed. DMSO was used to dissolve the purple formazan and the optical density (OD) value was measured at λ=490 nm using a BioTek ELx800 plate reader (BioTek Instruments, Inc.). The inhibition rate and 50% inhibitory concentration (IC_{50}) of diosgenin at each concentration was calculated. Inhibition rate and IC_{50} were calculated using the following formula: Inhibition rate (%) = [(Negative control group-Experimental group)/Negative control group] x 100.

Scratch test for the detection of cell migration. Cells in the logarithmic growth phase were prepared at $1x10^5$ cells/ml and transferred to a 6-well plate, and the corresponding diosgenin containing medium, MG63 (80 μM) and U2OS (40 μM), was added. The next day, when the cell confluence was >60%, a sterile pipette tip was used to evenly scratch the 6-well plate. The floating cells were washed away with PBS, and serum-free medium was used for culture in a cell culture incubator. After 24 h, the cells were imaged (magnification, x100), and the cell wound healing area was measured using Adobe Photoshop CS6 (Adobe Systems Europe, Ltd.) using an Olympus IX51 light microscope (Olympus Corporation). Relative wound closure was calculated using the following formula: relative wound closure (%)= (0 h time point area-each time point by the area)/0 h time point area x 100.

Transwell invasion assay. Diosgenin was added to cells in the logarithmic growth phase (MG63, 80 μM; U2OS 40 μM). Matrigel was thawed at 4˚C overnight and diluted 1:2 using serum-free medium. In the upper chamber of the Transwell insert, 30 μl diluted Matrigel was added at 37˚C for 120 min. The cell density was adjusted to $5x10^5$ cells/ml using serum-free medium. A total of 100 μl of the cells at a concentration of $5x10^5$ cells/ml was added to the upper chamber of a Transwell insert and 500 μl complete medium supplemented with 20% FBS was added to the lower chamber. The cells were then cultured in an incubator at 37˚C and 5% CO_2. After 24 h, the chamber was removed, washed with PBS, fixed in absolute ethanol for 20 min at 37˚C, stained with crystal violet for 20 min at 37˚C, washed with PBS and air-dried. An inverted microscope was used for observation, and the transmembrane cells in each group were counted using an Olympus IX51 light microscope.

Immunofluorescence assay for the observation of protein expression changes. Cells in the logarithmic growth phase were harvested and plated at a density of $5x10^4$ cells/ml. Diosgenin was added to each cell line (MG63, 80 μM; U2OS, 40 μM) and cultured for 24 h, after which the cells were air dried at room temperature (20˚C), fixed with 4% paraformaldehyde for 30 min at 20˚C, and subsequently washed with PBS three times. Two drops of a 3% H_2O_2-methanol solution and 75 μl ready-to-use goat serum (cat. no. AR0009; Wuhan Boster Biological Technology, Ltd.) were added dropwise and then incubated for 20 min at room temperature. The primary antibodies used were rabbit anti-human TGF-β1 (cat. no. KG22744-1; dilution, 1:100; Nanjing KeyGen Biotech Co., Ltd.) and incubated for 2 h at 37˚C, after which the samples were washed with PBS three times. A FITC-conjugated secondary antibody (1:200 dilution) was added and incubated for 1 h in the dark at 37˚C, and the samples were washed with PBS three times. After dropwise addition of a DAPI solution 0.2 μg/ml, antiquench

gel (cat. no. KGF028; Nanjing KeyGen Biotech Co., Ltd.) was used for mounting. A total of three high-expression regions of the cells were observed under a fluorescence microscope and photographed for preservation. The integrated optical density (IOD) under the field of view was calculated using Image-Pro Plus version 6.0 (Media Cybernetics, Inc.), and the mean density was calculated as mean density = IOD/area of the field.

Western blotting for the detection of protein expression. Cells in the logarithmic growth phase were harvested and plated at a density of $5x10^5$ cells/ml. The following day, after the cells had adhered to the wells, the medium was replaced and diosgenin was added to each cell line (MG63, 80 μM; U2OS, 40 μM). In the SB203580 group, SB203580 (cat. no. KGR0067 Nanjing KeyGen Biotech Co., Ltd.) was co-cultured with cells for 1 h. After 24 h, total cellular protein was extracted using a total protein extraction kit (cat. no. KGP250; Nanjing KeyGen Biotech Co., Ltd.), and the protein concentration was measured with a bicinchoninic acid protein concentration assay kit. Proteins were resolved for 90 min by 10% SDS-PAGE (30 μg/well). The resolved proteins were transferred to PVDF membranes using a Bio-Rad semidry transfer system (Bio-Rad Laboratories, Inc.). The PVDF membrane was subsequently blocked with 5% skimmed milk powder overnight at 4˚C and then incubated with the primary antibody overnight at 4˚C. The following primary antibodies were used: Rabbit anti-human E-cadherin (cat. no. KG22195-2; 1:200); rabbit anti-human vimentin (cat. no. KG22794-2; 1:200); rabbit anti-human ERK1/2 (cat. no. KG30107-2; 1:200); rabbit anti-human jun N-terminal kinase (JNK) 1/2 (cat. no. KG22481-2; 1:200); rabbit anti-human P38 (cat. no. KG30244-2; 1:200); rabbit anti-human pERK1/2 (cat. no. KG30246-2; 1:200); rabbit anti-human pJNK1/2 (cat. no. KG11504-2; 1:200); and rabbit anti-human pP38 (cat. no. KG11253-2; 1:200). The secondary antibodies used were goat anti-rabbit immunoglobulin G (IgG; cat. no. KGAA25; 1:200) and goat anti-mouse IgG (cat. no. KGAA37; 1:4,000). Both the primary and secondary antibodies were obtained from Nanjing KeyGen Biotech Co., Ltd. The following day, the membrane was incubated with the corresponding secondary antibody (1:4,000) for 1 h at room temperature, and the signal was visualized using enhanced chemiluminescent reagent (cat. no. KGP1121; Nanjing KeyGen Biotech Co., Ltd.). A gel imager and Gel-Pro32 version 4.4.0.36 (Bio-Rad, Inc.) were used for collecting images and analyzing the gray scale values relative to the GAPDH signal.

Reverse transcription-quantitative PCR (RT-qPCR). Cells in the logarithmic growth phase were harvested and digested with 0.25% trypsin and a trypsin digestive solution containing 0.02% EDTA to prepare a single-cell suspension. Subsequently 1 ml TRIzol® (Invitrogen; Thermo Fisher Scientific, Inc.) and 200 μl chloroform were added, incubated at 4˚C for 10 min, mixed gently and centrifuged at centrifuged at 12,000 x g for 5 min at 4˚C. The supernatant was transferred to a new microcentrifuge tube. A total 800 μl precooled methanol (4˚C) was added, and the samples were placed at 4˚C for 5 min with gentle agitation. The supernatant was aspirated and discarded after centrifugation at 12,000 x g for 10 min at 4˚C. Subsequently, 1 ml precooled 75% ethanol (4˚C) was added, and the sample was centrifuged at 12,000 x g for 5 min at 4˚C. The supernatant was aspirated and discarded, and 30 μl diethyl pyrocarbonate water was added and dissolved at 4˚C for 5 min. RNA was prepared for storage in a -70˚C freezer. A total of 5 μl RNA sample and 495 μl 1X Tris-EDTA buffer were mixed. The concentration and purity of the RNA were determined by measuring the absorption values at 260 and 280 nm. An OD260/OD280 of 1.8-2.0 was considered to indicate RNA of good quality that could be used for subsequent experiments. The extracted RNA was reverse transcribed into cDNA using a First Strand cDNA Synthesis kit (Thermo Fisher Scientific, Inc.) using the following incubation conditions: 25˚C for 5 min, 42˚C for 60 min, and on ice for 5 min. Next, qPCR was performed using a fluorescence qPCR instrument (ABI StepOne Plus; Thermo Fisher Scientific, Inc.). Primers were synthesized by Jiangsu Health Vocational College. The primer sequences were: GAPDH (90 bp) forward, 5-AGATCA TCAGCAATGCCTCCT-3 and reverse, 5-TGAGTCCTTCCA CGATACCAA-3; and E-cadherin (108 bp) forward, 5-CCA AGCAGCAGTACATTCTACA-3 and reverse, 5-CATTCA CATCCAGCACATCCA-3. The amplification conditions were as follows: Predenaturation at 95˚C for 3 min, followed by 45 cycles of denaturation at 95˚C for 10 sec, annealing at 60˚C for 20 sec and extension at 72˚C for 35 sec. The specificity of the amplified products was monitored by a dissolution curve. Relative gene expression was analyzed and calculated using the $2^{-\Delta\Delta Cq}$ method (30), and the expression levels of the target genes were normalized to GAPDH (ABI StepOne version 2.3; Applied Biosystems; Thermo Fisher Scientific, Inc.).

Statistical analysis. All the data are presented as the mean ± standard deviation and experiments were performed in triplicate. Statistical analyses were performed in SPSS software version 16.0 (SPSS, Inc.). Statistical comparisons between two groups were performed using an unpaired Student's t-test and comparisons between multiple groups were performed using a one-way ANOVA followed by a post hoc Tukey's test. $P<0.05$ was considered to indicate a statistically significant difference.

Results

Diosgenin inhibits the proliferation of osteosarcoma MG63 and U2OS cells. MG63 and U2OS cells were treated with diosgenin at different molar mass concentrations (200, 100, 50, 25, 12.5 and 6.25 μM) for 24 h. The results shown in Fig. 1 revealed that diosgenin had inhibitory effects on both cell lines in a dose-dependent manner. The 24-h IC_{50} of this drug in MG63 and U2OS cells were 76.2 and 40.15 μM, respectively.

Diosgenin inhibits the migratory ability of osteosarcoma cells. The cell scratch test is a method for detecting cell movement and can be used to detect the invasive and metastatic capacities of tumor cells (31). Fig. 2 shows that relative wound closure (%) of the MG63 cells in the control group were 34.03±3.42 and 77.45±4.50 after 12 and 24 h, respectively, while relative wound closure (%) of the U2OS cells in the control group were 48.16±3.18 and 67.71±4.22, respectively. However, upon treatment with the IC_{50} dose of diosgenin, relative wound closure (%) of MG63 cells (80 μM) were 18.83±2.61 and 28.75±2.11 after 12 and 24 h, respectively. Similarly, when U2OS cells were treated with 40 μm diosgenin, relative wound closure (%) were

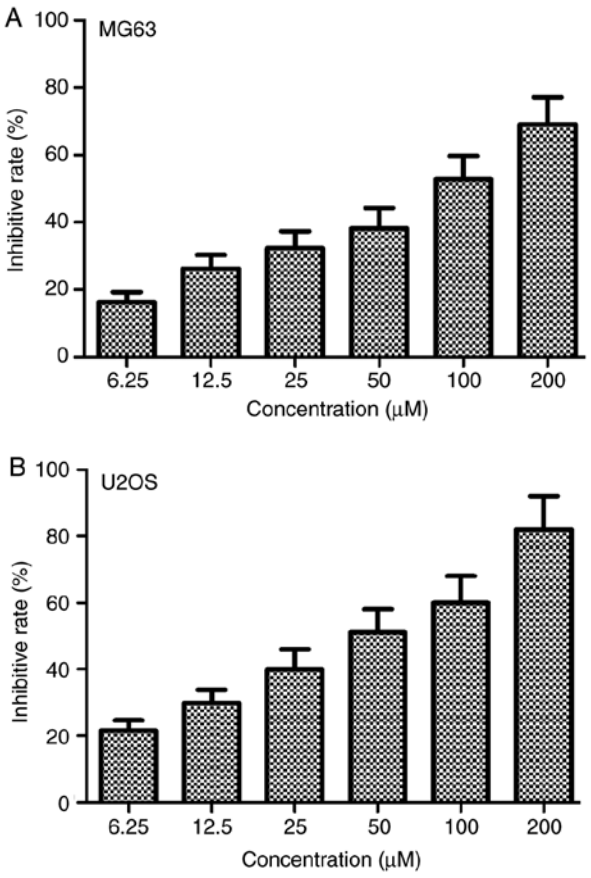

Figure 1. Effect of diosgenin on the proliferation of MG63 and U2OS osteosarcoma cells. Inhibitory effect of diosgenin at different concentrations on (A) MG63 and (B) and U2OS cells.

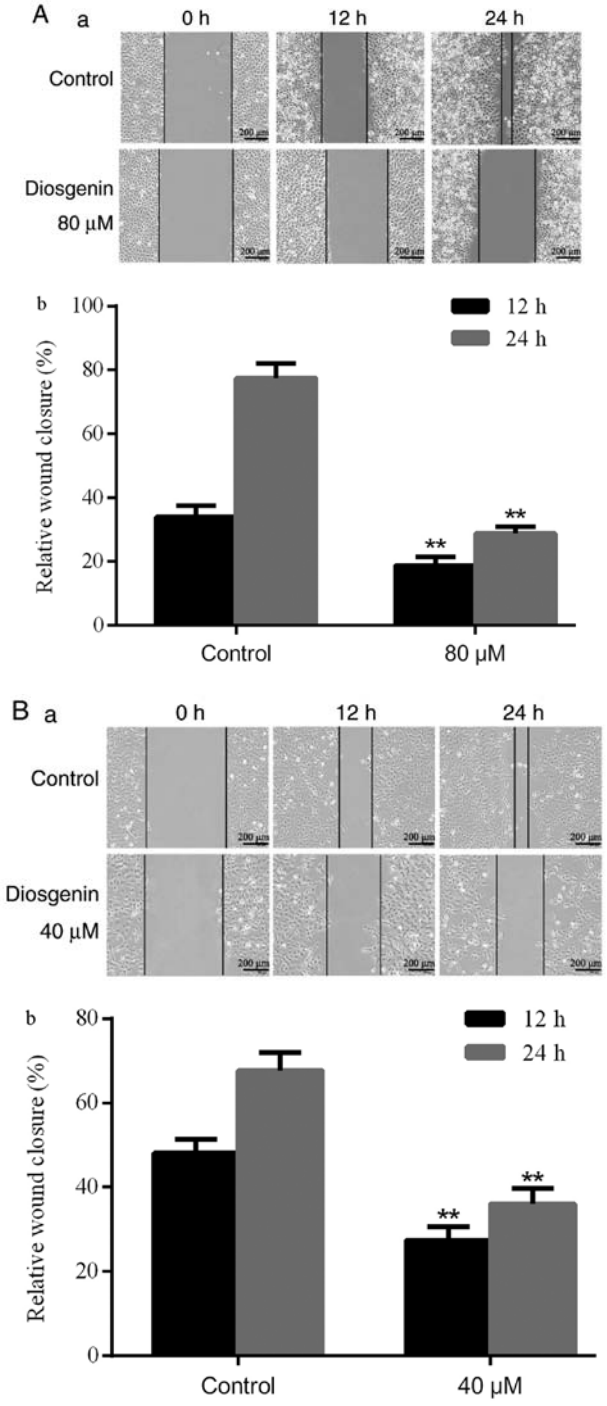

Figure 2. Effect of diosgenin on migration of osteosarcoma cells. Migratory ability of (A-a) MG63 and (B-a) U2OS osteosarcoma cells 12 and 24 h after administration of an IC_{50} dose of diosgenin. The grey area in (A-a) and (B-a) was the scratched area. Quantification of relative wound closure (%) in (A-b) MG63 and (B-b) U2OS cells. Compared with the control group, the rate of relative wound closure in MG63 and U2OS cells was decreased following treatment with diosgenin. Magnification, x100. **P<0.01.

27.36±3.26 and 36.02±3.74, respectively. Compared to those of the cells in the control group, the *in vitro* migratory abilities of the two types of osteosarcoma cells in the group treated with diosgenin were decreased (P<0.01).

Diosgenin inhibits osteosarcoma cell invasion. We next employed a Transwell test, which detects the invasive ability of cells based on their ability to pass through Matrigel (32). As shown in Fig. 3, the number of MG63 cells passing through the Matrigel after 12 and 24 h in the control group was 97±2.59 and 122±1.58/field of view, respectively. For U2OS cells, the counts were 84.2±3.27 and 204.6±2.51/field of view, respectively. However, the numbers of MG63 cells passing through the Matrigel after 12 and 24 h in the drug-treated group was only 41±2.07 and 53±1.82/field of view, respectively, and the number of U2OS cells was 45.4±2.7 and 55.6±2.3/field of view, respectively. Compared with that of the respective control for each cell line, the invasive ability of the diosgenin-treated osteosarcoma cells was decreased (P<0.05).

Diosgenin inhibits TGF-β1 protein expression in the osteosarcoma cell lines. As shown in Fig. 4, following treatment with diosgenin, the ODs were 1.25±0.03 and 1.07±0.04/pixel in the MG63 and U2OS cells, respectively. Compared with the respective control group, the average TGF-β1 ODs of MG63 and U2OS cells were 1.33±0.02 and 1.25±0.04/pixel. TGF-β1 protein expression in the two treated osteosarcoma cell line groups was decreased (P<0.05).

Diosgenin downregulates TGF-β1 and upregulates E-cadherin protein expression in in the osteosarcoma cell lines. To determine whether the effect of diosgenin on the invasion and migration of the two osteosarcoma cell lines was associated with

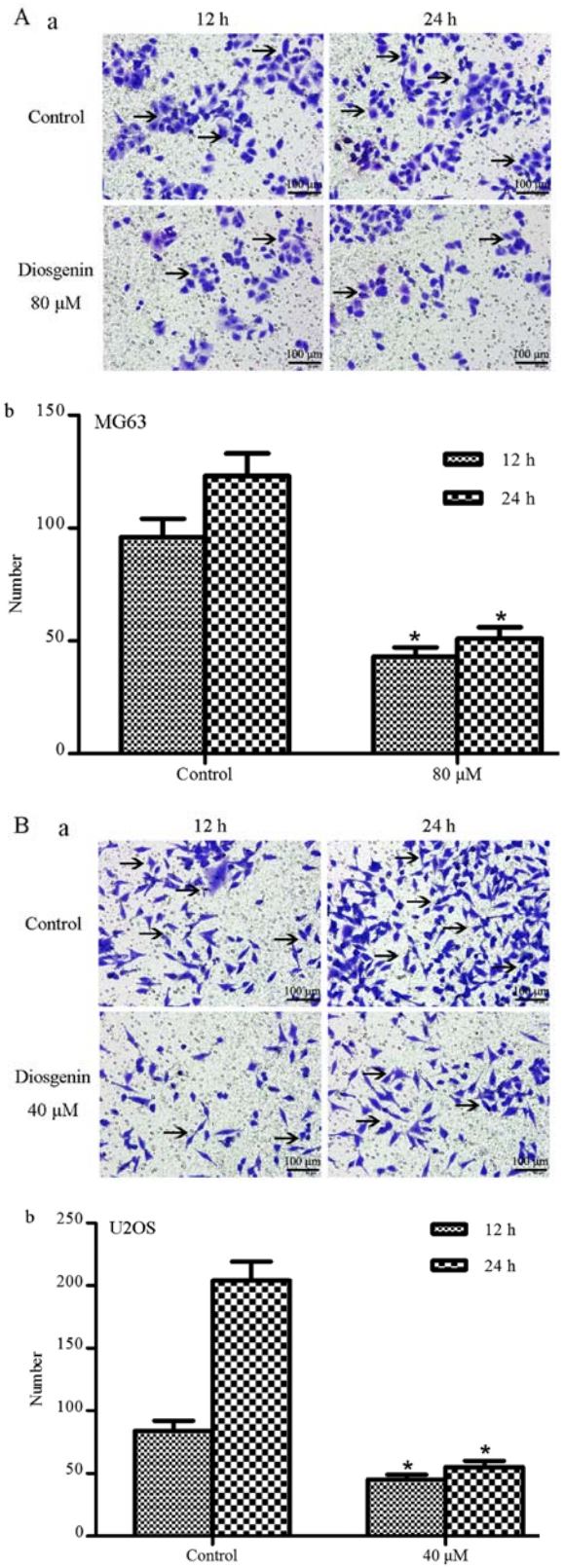

Figure 3. Effect of diosgenin on the invasion of osteosarcoma cells. Effect of diosgenin at an IC_{50} dose on (A-a) MG63 and (B-a) U2OS cells. Count of the cells that had passed through the Matrigel at 12 and 24 h following the administration of diosgenin to (A-b) MG63 and (B-b) U2OS cells. Magnification, x200. *P<0.05 compared with time respective control.

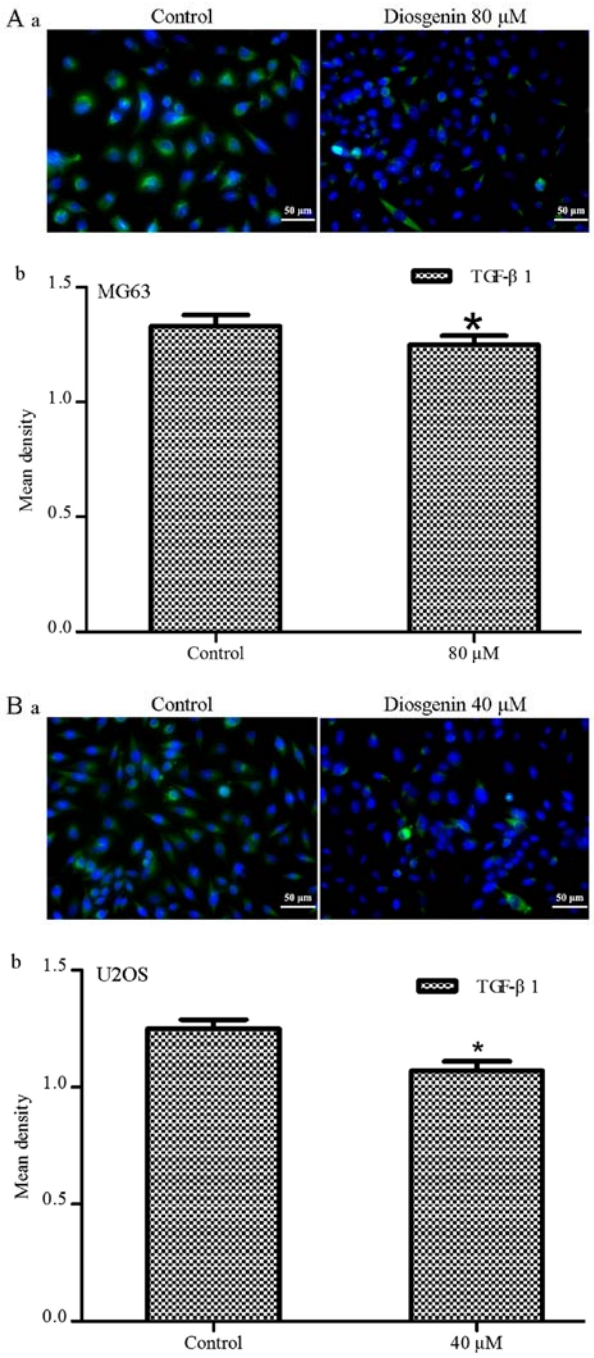

Figure 4. Diosgenin inhibits TGF-β1 protein expression in osteosarcoma cells. Fluorescence images of the effect of diosgenin on (A-a) MG63 and (B-a) U2OS cells. The green fluorescence in the figure represents the level of the TGF-β1 protein. Quantitative analysis of TGF-β1 immunofluorescence in (A-b) MG63 and (B-b) U2OS cells. Magnification, x400. *P<0.05. TGF-β1, transforming growth factor β1.

EMT, western blotting was used to detect changes in TGF-β1, E-cadherin and vimentin protein expression in the osteosarcoma cell lines prior to and following diosgenin administration. As shown in Fig. 5, after diosgenin treatment, the protein expression levels of TGF-β1 were decreased, while those of E-cadherin were increased in both cell types (P<0.01), suggesting that the invasive and migratory capacities of the cells were inhibited. However, diosgenin had no effect on vimentin protein expression.

Diosgenin inhibits the ERK/JNK/P38 signaling pathway in the osteosarcoma cell lines. Western blot analysis was used to assess the ERK/JNK/P38 pathway in the osteosarcoma cell

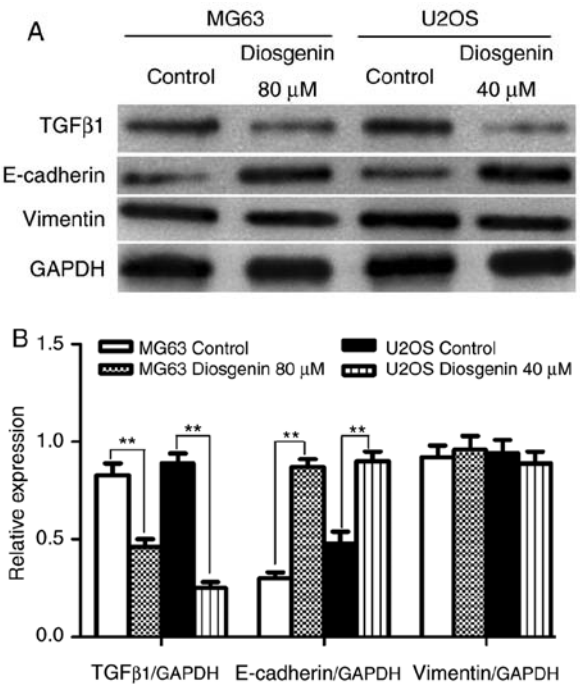

Figure 5. Western blot analysis of the effects of diosgenin on the expression of TGF-β1, E-cadherin and vimentin. (A) Western blot of TGF-β1, E-cadherin and vimentin. (B) Quantification of expression relative to GAPDH. Treatment with diosgenin significantly decreased TGF-β1 expression, increased E-cadherin expression and did not affect vimentin expression. **P<0.01. TGF β1, transforming growth factor β1.

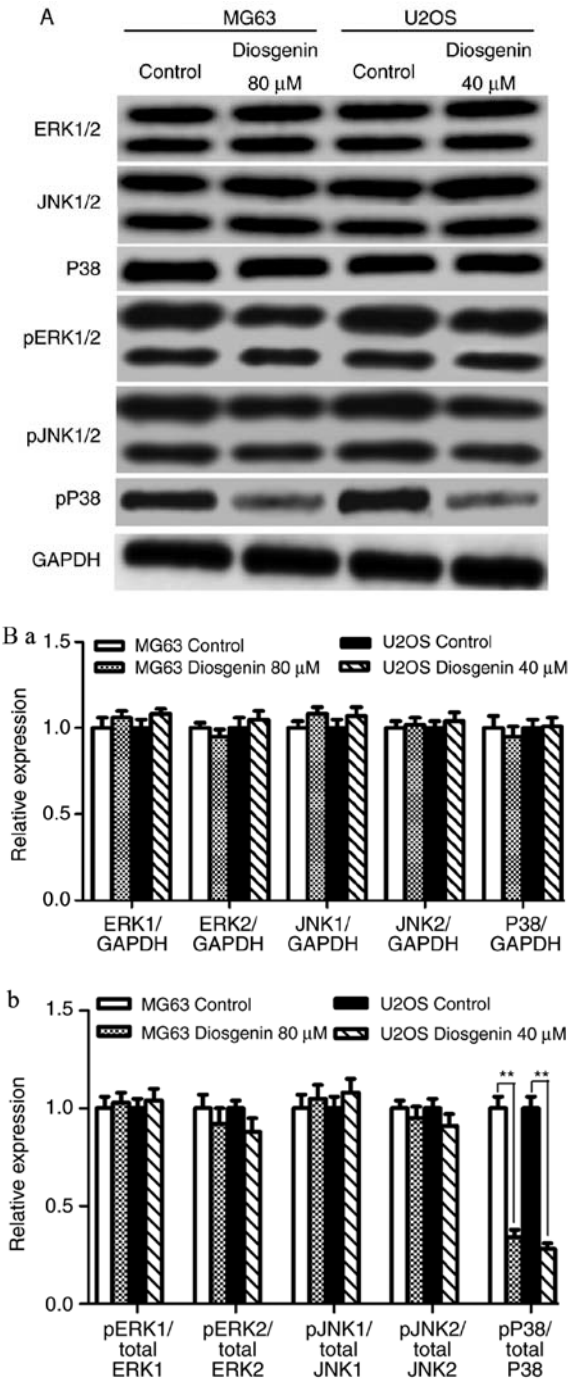

Figure 6. Western blot analysis of the effects of diosgenin on the expression of ERK1/2, JNK1/2, P38 and pP38. (A) Western blot analysis of ERK1/2, JNK1/2, P38, pERK1/2 and pJNK1/2 in the osteosarcoma cell lines prior to and following diosgenin treatment. (B-a) Quantification of expression in ERK1/2, JNK1/2, P38 relative to GAPDH. (B-b) Quantification of expression levels in pERK1/2, pJNK1/2, pP38 relative to total ERK1/2, total JNK1/2, total P38. There was a significant reduction in the quantity of pP38, although the levels of total P38 were not affected by diosgenin treatment. **P<0.01. ERK1/2, extracellular signal-regulated kinase; JNK, c Jun N-terminal kinase; p, phospho.

lines before and after diosgenin treatment. As shown in Fig. 6, among the ERK/JNK/P38 pathway molecules, only the pP38 protein exhibited a decreased level in both osteosarcoma cell lines following administration of diosgenin (P<0.01), while changes in the levels of other proteins in the pathway were not statistically significant.

Diosgenin inhibits the invasion and migration of the two osteosarcoma cell lines by reducing the protein expression levels of the pP38 in the MAPK pathway. Diosgenin treatment was combined with a pP38 protein inhibitor and the expression levels of a downstream indicator of EMT, E-cadherin was observed (33). As shown in Fig. 7, the cellular expression level of E-cadherin in the group treated with the pP38 inhibitor SB203580 (20 μM) was not statistically different compared with the control group; however, the expression level of E-cadherin in the osteosarcoma cell lines treated with diosgenin in combination with SB203580 group was decreased compared with the cells in the diosgenin group (MG63, P<0.05; U2OS, P<0.01).

Discussion

In the present study, an MTT assay was used to determine the IC_{50} dose of diosgenin on the MG63 and U2OS cell lines. The MTT assay also demonstrated that the drug had a concentration-dependent inhibitory effect on the proliferation of both osteosarcoma cell lines.

A wound healing and Transwell assay was used to observe the effect of diosgenin on migration and invasion in the osteosarcoma cells at 12 and 24 h after diosgenin administration and confirmed that the invasive and migratory abilities of these osteosarcoma cells were decreased to different degrees upon diosgenin administration in a time-dependent manner.

TGF-β is a protein widely recognized for its role in EMT regulation (34). It primarily regulates downstream transcription factors through both Smad-dependent and Smad-independent

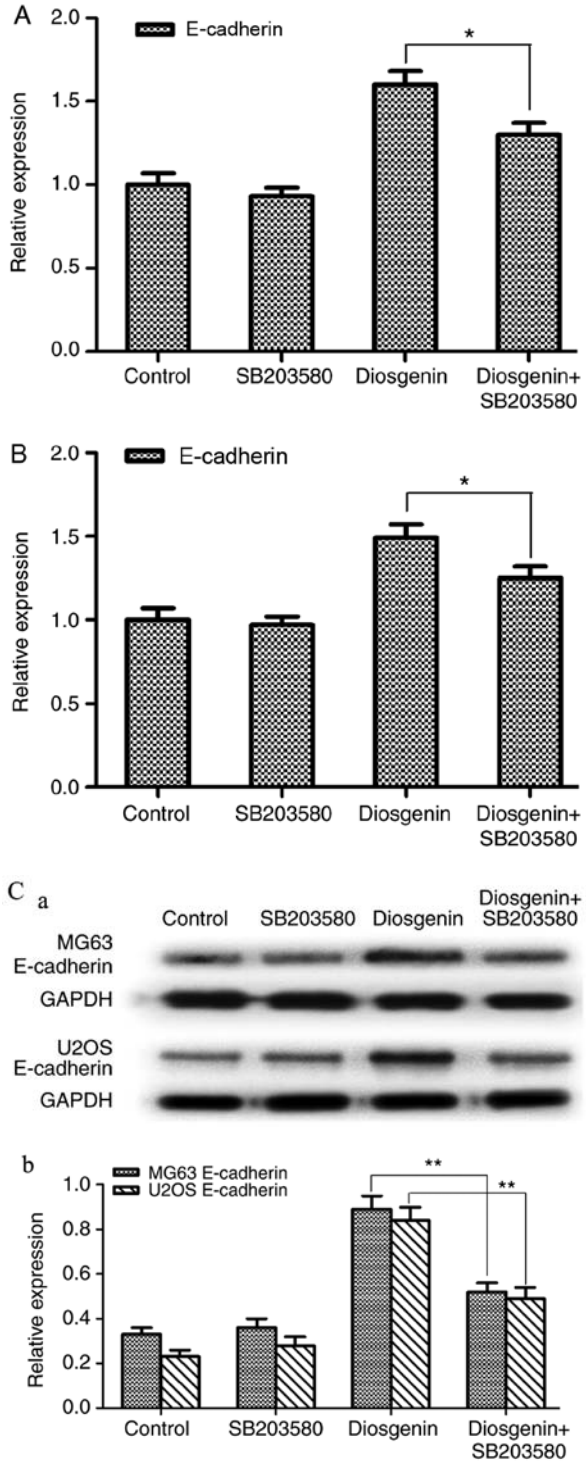

Figure 7. Treatment with diosgenin and the P38 pathway inhibitor SB203580 on E-cadherin expression. Following treatment with the mitogen-activated protein kinase pathway pP38 inhibitor SB203580 combined with diosgenin, the changes in E-cadherin expression were determined by reverse transcription quantitative PCR in the (A) MG63 and (B) U2OS. (C-a) Western blot analysis of E-cadherin protein expression in osteosarcoma cells MG63 and U2OS after treatment with diosgenin combined with pP38 inhibitor SB203580. (C-b) Quantification of expression levels relative to GAPDH. In both cell lines, both at the mRNA and protein expression levels, Treatment with the pP38 inhibitor significantly decreased E-cadherin expression compared with diosgenin alone. *P<0.05, **P<0.01. p, phospho.

signaling pathways and thereby participates in the regulation of EMT (35). TGF-β was one of the first factors discovered to be able to induce EMT in tumor cells (36). There are three primary subtypes, TGF-β1-3, and among these, the TGFβ1 has been reported to be associated with EMT initiation (37). TGF β1 can promote the metastasis of tumor cells in the late stage of tumor cell growth, and its cancer-promoting effects usually occur at the same time as the induction of tumor cell EMT (38). A number of experiments have shown that the levels of TGF-β1 in tumor cells are positively correlated with the promotion of tumor cell migration and invasion (39-41). However, TGF-β-induced apoptosis and EMT may be independent cellular events that are mutually exclusive but associated with each other and occur on a similar timeframe (42).

E-cadherin is the primary molecule that maintains the polarity and intercellular adhesion of epithelial cells. Its primary function is to form a protein complex which links to the actin cytoskeleton and prevents the metastasis and invasion of tumor cells (43). However, EMT can reduce or eliminate the expression of epithelial cell adhesion molecules and cytoskeletal components to achieve a stromal cell phenotype. Therefore, the reduction or loss of E-cadherin expression is an important marker for EMT initiation in tumor cells (44). Experiments have shown that a decrease in the E-cadherin protein level can promote invasion and metastasis in tumor cells (45-47).

Vimentin belongs to a family of cellular intermediate filament proteins and is an important component of the cytoskeleton. Studies have found that tumor cells can exhibit high invasiveness and strong migratory abilities when vimentin is highly expressed, whereas these abilities are reduced after knocking out or reducing vimentin levels in these cells (48,49). In some invasive tumors, such as colon cancer, prostate cancer and breast cancer, the expression of vimentin is also positively correlated with the degree of malignancy of the tumor (50-52).

To determine whether the ability of diosgenin to inhibit invasion and migration in osteosarcoma cells was associated with EMT, TGF-β1 expression was analyzed using immunofluorescence prior to and following treatment. TGF-β1 expression decreased to varying degrees in the two osteosarcoma cell lines following treatment with diosgenin. To further observe whether the effects of diosgenin were associated with EMT and to simultaneously verify the results of the immunofluorescence experiment, western blotting was used to measure the expression levels of three proteins associated with EMT which showed that diosgenin reduced the protein expression levels of TGF-β1 and increased those of E-cadherin but had no effect on vimentin. These results suggested that diosgenin may inhibit the initiation of EMT in osteosarcoma cells by reducing TGF β1 protein expression levels and increasing E-cadherin protein levels.

The MAPK signaling pathway is one of the numerous molecular signaling pathways that can affect the initiation of EMT (53). It has a synergistic effect with TGF-β in the initiation of EMT in tumor cells. The ERK, JNK and P38 proteins in the MAPK signaling pathway are key factors for initiation of EMT (54). It has been shown that once phosphorylated, these three MAPK pathway proteins can bind to the serine and threonine sites of Smad2/3-linked polypeptide, thereby promoting the activation of the Smad pathway and initiating EMT in tumor cells (55). The tumor cells can thereby become more migratory and invasive (56). In addition, elevating ERK

phosphorylation can upregulate TGF-β1 protein levels in tumor cells. ERK phosphorylation is one of the primary drivers of EMT in tumor cells *in vitro* (57); in addition, TGF-β1 can activate TGF-β-activated kinase 1, which promotes the phosphorylation of P38 and further drives EMT (58).

In the present study, all the proteins associated with the MAPK signaling pathway were analyzed by western blotting and it was demonstrated that diosgenin had no effect on the total ERK1/2, JNK1/2 and P38 protein levels in the two osteosarcoma cell lines. Diosgenin also did not significantly alter the levels of phosphorylated ERK1/2 or JNK1/2. However, diosgenin did decrease the levels of pP38. Therefore, diosgenin may have inhibited the MAPK signaling pathway in both osteosarcoma cell lines by decreasing the protein expression levels of pP38.

However, the MAPK signaling pathway is involved in a number of functions associated with cancerous behaviors. In addition to the initiation of EMT, the MAPK signaling pathway additionally serves roles in cell growth, apoptosis and inflammation (58-61). A previous study has shown that diosgenin can inhibit the cell cycle of osteosarcoma cells through the P38 protein (62). To confirm that the observed diosgenin-mediated inhibition of the MAPK pathway in osteosarcoma cells was associated with EMT, cells were treated with a combination of an inhibitor of the p38MAPK pathway with diosgenin treatment, and the levels of E-cadherin, a downstream EMT molecule, were measured by RT-qPCR and western blotting. The results showed that the E-cadherin levels in osteosarcoma cells were decreased after diosgenin administration in combination with the pathway inhibitor. The above experiments thus suggested that the pP38 protein was a target of diosgenin-mediated inhibition of EMT initiation in osteosarcoma cells.

In conclusion, the present study examined the ability of diosgenin to inhibit the invasion and migration of two different osteosarcoma cell lines *in vitro* and confirmed that this drug can inhibit EMT initiation in osteosarcoma cells by decreasing TGF-β1 expression and increasing E-cadherin protein levels. Additionally, the MAPK signaling pathway was involved in the diosgenin-mediated inhibition of EMT in osteosarcoma cells. The target of this drug was the pP38 protein in the MAPK signaling pathway. As a highly efficient plant extract with low toxicity, diosgenin may have utility as an auxiliary drug for the clinical reduction of osteosarcoma metastasis.

Acknowledgements

Not applicable.

Funding

The present study was supported by the Natural Science Foundation of Jiangsu Province (grant no. SBK2019020703), Wuxi Science and Technology Development Project (grant no. CSZ0N1619) and Qinglan Project of Excellent Teaching Team in Jiangsu (grant no. TD2019).

Availability of data and materials

The datasets used and/or analyzed during the present study is available from the corresponding author on reasonable request.

Authors' contributions

LZ supervised and directed this study. HH and LZ performed the majority of the experiments. LZ contributed to the conception and design of the experiments the project design. CN and JZ contributed to the cell culture and RNA extraction. XQ helped with interpretation of data for the experiments. CN analyzed the data and H wrote this manuscript. All authors read and approved the manuscript and agree to be accountable for all aspects of the research in ensuring that the accuracy or integrity of any part of the work are appropriately investigated and resolved.

Ethics approval and consent to participate

Not applicable.

Patient consent for publication

Not applicable.

Competing interests

The authors declare that they have no competing interests.

References

1. Anderson ME: Update on survival in osteosarcoma. Orthop Clin North Am 47: 283-292, 2016.
2. Fujiwara T, Oda M, Yoshida A, Ogura K, Chuman H, Kusumoto M and Kawai A: Atypical manifestation of lung metastasis 17 years after initial diagnosis of low-grade centralosteosarcoma. J Orthop Sci 22: 357-361, 2017.
3. Zhang Y, He Z, Li Y, Yang Y, Shi J, Liu X, Yuan T, Xia J, Li D, Zhang J and Yang Z: Selection of surgical methods in the treatment of upper tibia osteosarcoma and prognostic analysis. Oncol Res Treat 40: 528-532, 2017.
4. Deng ZP, Liu BY, Sun Y, Jin T, Li B, Ding Y and Niu XH: Transition from tumor tissue to bone marrow in patients with appendicular osteosarcoma after neoadjuvant chemotherapy. Chin Med J (Engl) 130: 2215-2218, 2017.
5. Zhao K, Yang SY, Geng J, Gong X, Gong W, Shen L and Ning B: Combination of anginex gene therapy and radiation decelerates the growth and pulmonary metastasis of human osteosarcoma xenografts. Cancer Med 7: 2518-2529, 2018.
6. Fenger JM, London CA and Kisseberth WC: Canine osteosarcoma: A naturally occurring disease to inform pediatric oncology. ILAR J 55: 69-85, 2014.
7. Zhang Y, Hu Q, Li G, Li L, Liang S, Zhang Y, Liu J, Fan Z, Li L, Zhou B, *et al*: ONZIN upregulation by mutant p53 contributes to osteosarcoma metastasis through the CXCL5-MAPK signaling pathway. Cell Physiol Biochem 48: 1099-1111, 2018.
8. Zhuo B, Li Y, Gu F, Li Z, Sun Q, Shi Y, Shen Y, Zhang F, Wang R and Wang X: Overexpression of CD155 relates to metastasis and invasion in osteosarcoma. Oncol Lett 15: 7312-7318, 2018.
9. Liu P, Yang P, Zhang Z, Liu M and Hu S: Ezrin/NF-κB pathway regulates EGF-induced epithelial-mesenchymal transition (EMT), metastasis, and progression of osteosarcoma. Med Sci Monit 24: 2098-2108, 2018.
10. Chen Y, Tang YM, Yu SL, Han YW, Kou JP, Liu BL and Yu BY: Advances in the pharmacological activities and mechanisms of diosgenin. Chin J Nat Med 13: 578-587, 2015.
11. Yan W, Ji L, Hang S and Shun Y: New ionic liquid-based preparative method for diosgenin from *Rhizoma dioscoreae* nipponicae. Pharmacogn Mag 9: 250-254, 2013.
12. Kiasalari Z, Rahmani T, Mahmoudi N, Baluchnejadmojarad T and Roghani M: Diosgenin ameliorates development of neuropathic pain in diabetic rats: Involvement of oxidative stress and inflammation. Biomed Pharmacother 86: 654-661, 2017.
13. Hua S, Li Y, Su L and Liu X: Diosgenin ameliorates gestational diabetes through inhibition of sterol regulatory element-binding protein-1. Biomed Pharmacother 84: 1460-1465, 2016.

14. Wei Z, Xin G, Wang H, Zheng H, Ji C, Gu J, Ma L, Qin C, Xing Z, Niu H and Huang W: The diosgenin prodrug nanoparticles with pH-responsive as a drug delivery system uniquely prevents thrombosis without increased bleeding risk. Nanomedicine 14: 673-684, 2018.
15. Huang CH, Wang CC, Lin YC, Hori M and Jan TR: Oral administration with diosgenin enhances the induction of intestinal T helper 1-like regulatory T cells in a murine model of food allergy. Int Immunopharmacol 42: 59-66, 2017.
16. Wang YJ, Pan KL, Hsieh TC, Chang TY, Lin WH and Hsu JT: Diosgenin, a plant-derived sapogenin, exhibits antiviral activity in vitro against hepatitis C virus. J Nat Prod 74: 580-584, 2011.
17. Pons-Fuster López E, Wang QT, Wei W and López Jornet P: Potential chemotherapeutic effects of diosgenin, zoledronic acid and epigallocatechin-3-gallate on PE/CA-PJ15 oral squamous cancer cell line. Arch Oral Biol 82: 141-146, 2017.
18. Bhuvanalakshmi G, Basappa, Rangappa KS, Dharmarajan A, Sethi G, Kumar AP and Warrier S: Breast cancer stem-like cells are inhibited by diosgenin, a steroidal saponin, by the attenuation of the Wnt β-catenin signaling via the Wnt antagonist secreted frizzled related protein-4. Front Pharmacol 8: 124, 2017.
19. Nie C, Zhou J, Qin X, Shi X, Zeng Q, Liu J, Yan S and Zhang L: Diosgenin-induced autophagy and apoptosis in a human prostate cancer cell line. Mol Med Rep 14: 4349-4359, 2016.
20. Cai B, Liao A, Lee KK, Ban JS, Yang HS, Im YJ and Chun C: Design, synthesis of methotrexate-diosgenin conjugates and biological evaluation of their effect on methotrexate transport-resistant cells. Steroids 116: 45-51, 2016.
21. Ghosh S, More P, Derle A, Kitture R, Kale T, Gorain M, Avasthi A, Markad P, Kundu GC, Kale S, *et al*: Diosgenin functionalized iron oxide nanoparticles as novel nanomaterial against breast cancer. J Nanosci Nanotechnol 15: 9464-9472, 2015.
22. Ding W, Jiang Y, Jiang Y, Zhu T, Xu Y, Jiang W, Zhu W, Tang Z, Ge Z, Ma T and Tan Y: Role of SB203580 in the regulation of human esophageal cancer cells under the effection of diosgenin. Int J Clin Exp Med 8: 2476-2479, 2015.
23. Goossens S, Vandamme N, Van Vlierberghe P and Berx G: EMT transcription factors in cancer development re-evaluated: Beyond EMT and MET. Biochim Biophys Acta Rev Cancer 1868: 584-591, 2017.
24. Singh M, Yelle N, Venugopal C and Singh SK: EMT: Mechanisms and therapeutic implications. Pharmacol Ther 182: 80-94, 2018.
25. Cao Z, Livas T and Kyprianou N: Anoikis and EMT: Lethal 'Liaisons' during cancer progression. Crit Rev Oncog 21: 155-168, 2016.
26. Illam SP, Narayanankutty A, Mathew SE, Valsalakumari R, Jacob RM and Raghavamenon AC: Epithelial mesenchymal transition in cancer progression: Prev entive phytochemicals. Recent Pat Anticancer Drug Discov 12: 234-246, 2017.
27. Zahedi A, Phandthong R, Chaili A, Remark G and Talbot P: Epithelial-to-mesenchymal transition of A549 lung cancer cells exposed to electronic cigarettes. Lung Cancer 122: 224-233, 2018.
28. Wang X, Liang X, Liang H and Wang B: SENP1/HIF-1α feedback loop modulates hypoxia-induced cell proliferation, invasion and EMT in human osteosarcoma cells. J Cell Biochem 119: 1819-1826, 2018.
29. Chen Y, Zhang K, Li Y and He Q: Estrogen-related receptor α participates transforming growth factor-β (TGF-β) induced epithelial-mesenchymal transition of osteosarcoma cells. Cell Adh Migr 11: 338-346, 2017.
30. Livak KJ and Schmittgen TD: Analysis of relative gene expression data using real-time quantitative PCR and the 2(-Delta Delta C(T)) method. Methods 25: 402-408, 2001.
31. Wu J, Weng Y, He F, Liang D and Cai L: LncRNA MALAT-1 competitively regulates miR-124 to promote EMT and development of non-small-cell lung cancer. Anticancer Drugs 29: 628-636, 2018.
32. Chen C, Liang QY, Chen HK, Wu PF, Feng ZY, Ma XM, Wu HR and Zhou GQ: DRAM1 regulates the migration and invasion of hepatoblastoma cells via autophagy-EMT pathway. Oncol Lett 16: 2427-2433, 2018.
33. Cheng G, Gao F, Sun X, Bi H and Zhu Y: Paris saponin VII suppresses osteosarcoma cell migration and invasion by inhibiting MMP-2/9 production via the p38 MAPK signaling pathway. Mol Med Rep 14: 3199-3205, 2016.
34. Zhan L, Chen L and Chen Z: Knockdown of FUT3 disrupts the proliferation, migration, tumorigenesis and TGF-β induced EMT in pancreatic cancer cells. Oncol Lett 16: 924-930, 2018.
35. Kaur G, Li CG, Chantry A, Stayner C, Horsfield J and Eccles MR: SMAD proteins directly suppress PAX2 transcription downstream of transforming growth factor-beta 1 (TGF-β1) signalling in renal cell carcinoma. Oncotarget 9: 26852-26867, 2018.
36. David CJ, Huang YH, Chen M, Su J, Zou Y, Bardeesy N, Iacobuzio-Donahue CA and Massagué J: TGF-β tumor suppression through a lethal EMT. Cell 164: 1015-1030, 2016.
37. Chen CL, Chen YH, Tai MC, Liang CM, Lu DW and Chen JT: Resveratrol inhibits transforming growth factor-β2-induced epithelial-to-mesenchymal transition in human retinal pigment epithelial cells by suppressing the smad pathway. Drug Des Devel Ther 11: 163-173, 2017.
38. Huang TW, Li ST, Fang KM and Young TH: Hyaluronan antagonizes the differentiation effect of TGF-β1 on nasal epithelial cells through down-regulation of TGF-β type I receptor. Artif Cells Nanomed Biotechnol 46 (Suppl 3): S254-S263, 2018.
39. Duan W, Qian W, Zhou C, Cao J, Qin T, Xiao Y, Cheng L, Li J, Chen K, Li X, *et al*: Metformin suppresses the invasive ability of pancreatic cancer cells by blocking autocrine TGF-β1 signaling. Oncol Rep 40: 1495-1502, 2018.
40. Ohtani H, Terashima T and Sato E: Immune cell expression of TGFβ1 in cancer with lymphoid stroma: Dendritic cell and regulatory T cell contact. Virchows Arch 472: 1021-1028, 2018.
41. Tao Y, Sturgis EM, Huang Z, Wang Y, Wei P, Wang JR, Wei Q and Li G: TGFβ1 genetic variants predict clinical outcomes of HPV-positive oropharyngeal cancerpatients after definitive radiotherapy. Clin Cancer Res 24: 2225-2233, 2018.
42. Song J and Shi W: The concomitant apoptosis and EMT underlie the fundamental functions of TGF-β. Acta Biochim Biophys Sin (Shanghai) 50: 91-97, 2018.
43. Wang YP, Wang QY, Li CH and Li XW: COX-2 inhibition by celecoxib in epithelial ovarian cancer attenuates E-cadherin suppression through reduced Snail nuclear translocation. Chem Biol Interact 292: 24-29, 2018.
44. Li X, Chen H, Liu Z, Ye Z, Gou S and Wang C: Overexpression of MIST1 reverses the epithelial-mesenchymal transition and reduces the tμmorigenicity of pancreatic cancer cells via the Snail/E-cadherin pathway. Cancer Lett 431: 96-104, 2018.
45. Yang Y, Shen J, Yan D, Yuan B, Zhang S, Wei J and Du T: Euchromatic histone lysine methyltransferase 1 regulates cancer development in human gastric cancer by regulating E-cadherin. Oncol Lett 15: 9480-9486, 2018.
46. Zhu S, Deng S, He C, Liu M, Chen H, Zeng Z, Zhong J, Ye Z, Deng S, Wu H, *et al*: Reciprocal loop of hypoxia-inducible factor-1α (HIF-1α) and metastasis-associated protein 2 (MTA2) contributes to the progression of pancreatic carcinoma by suppressing E-cadherintranscription. J Pathol 245: 349-360, 2018.
47. Ma L, Liu L, Ma Y, Xie H, Yu X, Wang X, Fan A, Ge D, Xu Y, Zhang Q and Song C: The role of E-cadherin/β-catenin in hydroxysafflor yellow a inhibiting adhesion, invasion, migration and lung metastasis of hepatoma cells. Biol Pharm Bull 40: 1706-1715, 2017.
48. Karim NA, Eldessouki I, Yellu M, Namad T, Wang J and Gaber O: A case study in advanced lung cancer patients with vimentin over expression. Clin Lab 63: 1575-1579, 2017.
49. Noh H, Yan J, Hong S, Kong LY, Gabrusiewicz K, Xia X, Heimberger AB and Li S: Discovery of cell surface vimentin targeting mAb for direct disruption of GBM tumor initiating cells. Oncotarget 7: 72021-72032, 2016.
50. Lou L, Yu Z, Wang Y, Wang S and Zhao Y: c-Src inhibitor selectively inhibits triple negative breast cancer overexpressed vimentin in vitro and in vivo. Cancer Sci 109: 1648-1659, 2018.
51. Xu CY, Qin MB, Tan L, Liu SQ and Huang JA: NIBP impacts on the expression of E-cadherin, CD44 and vimentin in colon cancer via the NF-κB pathway. Mol Med Rep 13: 5379-5385, 2016.
52. Vyas AR and Singh SV: Functional relevance of D, L-sulforaphane-mediated induction of vimentin and plasminogen activator inhibitor-1 in human prostate cancer cells. Eur J Nutr 53: 843-852, 2014.
53. Huang M, Wang YP, Zhu LQ, Cai Q, Li HH and Yang HF: MAPK pathway mediates epithelial-mesenchymal transition induced by paraquat in alveolar epithelial cells. Environ Toxicol 31: 1407-1414, 2016.
54. Xiao K, Cao S, Jiao L, Song Z, Lu J and Hu C: TGF-β1 protects intestinal integrity and influences Smads and MAPK signal pathways in IPEC-J2 after TNF-α challenge. Innate Immun 23: 276-284, 2017.

55. Park JH, Yoon J, Lee KY and Park B: Effects of geniposide on hepatocytes undergoing epithelial-mesenchymal transition in hepatic fibrosis by targeting TGFβ/Smad and ERK-MAPK signaling pathways. Biochimie 113: 26-34, 2015.
56. Jiang Y, Wu C, Boye A, Wu J, Wang J, Yang X and Yang Y: MAPK inhibitors modulate Smad2/3/4 complex cyto-nuclear translocation in myofibroblasts via Imp7/8 mediation. Mol Cell Biochem 406: 255-262, 2015.
57. Kang HM, Park BS, Kang HK, Park HR, Yu SB and Kim IR: Delphinidin induces apoptosis and inhibits epithelial-to-mesenchymal transition via the ERK/p38 MAPK-signaling pathway in human osteosarcoma cell lines. Environ Toxicol 33: 640-649, 2018.
58. Wei J, Li Z, Chen W, Ma C, Zhan F, Wu W and Peng Y: AEG-1 participates in TGF-beta1-induced EMT through p38 MAPK activation. Cell Biol Int 37: 1016-1021, 2013.
59. Lyu Z, Cao J, Wang J and Lian H: Protective effect of vitexin reduces sevoflurane-induced neuronal apoptosis through HIF-1α, VEGF and p38 MAPK signaling pathway in vitro and in newborn rats. Exp Ther Med 15: 3117-3123, 2018.
60. Xiang S, Xiang T, Xiao Q, Li Y, Shao B and Luo T: Zinc-finger protein 545 is inactivated due to promoter methylation and functions as a tumor suppressor through the Wnt/β-catenin, PI3K/AKT and MAPK/ERK signaling pathways in colorectal cancer. Int J Oncol 51: 801-811, 2017.
61. Kello M, Kulikova L, Vaskova J, Nagyova A and Mojzis J: Fruit peel polyphenolic extract induced apoptosis in human breast cancer cells is associated with ROS production and modulation of p38MAPK/Erk1/2 and the Akt signaling pathway. Nutr Cancer 69: 920-931, 2017.
62. Long C, Chen J, Zhou H, Jiang T, Fang X, Hou D, Liu P and Duan H: Diosgenin exerts its tumor suppressive function via inhibition of Cdc20 in osteosarcoma cells. Cell Cycle 18: 346-358, 2019.